Letter to the Editor

Desmoplastic small round cell tumor: the report of two cases and literature analysis review of the radiological findings

Wenying Chen[1#^], Haimei Chen[1#], Chang Zhao[2], Sidong Xie[1], Jie Qin[1], Weimin Liu[1]

[1]Department of Radiology, The Third Affiliated Hospital of Sun Yat-sen University, Guangzhou, China; [2]Department of Pathology, The Third Affiliated Hospital of Sun Yat-sen University, Guangzhou, China

[#]These authors contributed equally to this work.

Correspondence to: Weimin Liu, Master; Jie Qin, Doctor. Department of Radiology, The Third Affiliated Hospital of Sun Yat-sen University, No. 600, Tianhe Road, Shipai Street, Tianhe District, Guangzhou 510000, China. Email: liuwm8@mail.sysu.edu.cn; qinjie@mail.sysu.edu.cn.

Keywords: Desmoplastic small round cell tumor; Wilms tumor 1 (WT1); Ewing sarcoma region 1 (EWSR1); case description

Submitted Dec 03, 2022. Accepted for publication Apr 30, 2023. Published online May 29, 2023.
doi: 10.21037/qims-22-1344
View this article at: https://dx.doi.org/10.21037/qims-22-1344

Background

Desmoplastic small round cell tumor (DSRCT) is a rare, unique, and highly malignant tumor that tends to occur in children and adolescents. There is an obvious gender preference, with a male to female ratio reaching 5 to 1 (1,2). It occurs predominantly in the abdominal pelvic cavity, spreads along the peritoneal surface, and very rarely appears in the lungs (3), salivary glands (4), heart (5), colon (6), bones (7) and gonads (8,9). DSRCT has an occult onset and rapid disease progression and is susceptible to implantable spread and blood and lymphatic metastasis, which most often occurs in the liver, followed by the lungs, lymph nodes, and bones (10). In this study, we retrospectively analyzed the two cases of patients with DSRCT admitted to our hospital from October 2016 to October 2021 and referred to the relevant literature in recent years, with the aim of improving the understanding of their clinical and imaging characteristics.

Case presentation

Clinical history

Case 1

A 9-year-old boy touched a mass in his abdomen 2 weeks prior to attending The Third Affiliated hospital of Sun Yat-sen University but complained of no other discomfort. Multiphase contrast-enhanced computed tomography (CT; Toshiba CT Aquilion; 64 slices; slice thickness, 3 mm) of the abdomen revealed a large mass in the left kidney, measuring approximately 129 mm × 95 mm × 161 mm, with heterogeneous density and multiple calcifications within it, showing significant heterogeneous enhancement. There were also multiple metastases in the abdominal lymph nodes and the liver (*Figure 1*). Thereafter, the patient also underwent whole-body fluorine 18 fluorodeoxyglucose positron emission tomography-computed tomography (^{18}F-FDG PET-CT), which showed a large left renal

^ ORCID: 0000-0001-8661-5310.

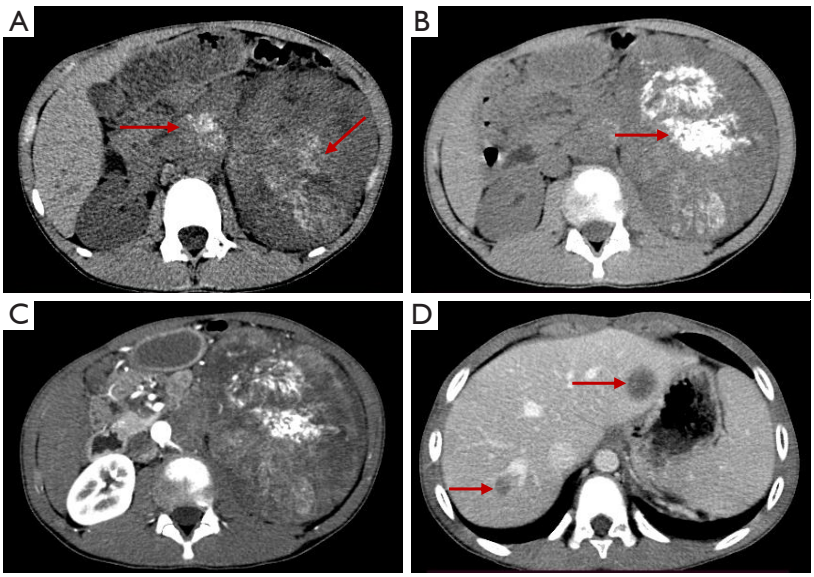

Figure 1 CT Results for case 1. (A) The image suggested a large mass in the left kidney compressing surrounding structures. The plain CT value of the solid component of the mass was about 36 HU, and the patchy calcification could be seen in the mass (right red arrow). In addition, the metastatic retroperitoneal lymph nodes were associated with calcification (left red arrow). (B) Extensive calcification and local necrosis were found in other layers of the mass (red arrow). (C) A contrast-enhanced scan showed uneven enhancement. The CT value after the enhanced scan was about 50–67 HU. (D) Multiple metastases in the liver (arrows). CT, computed tomography.

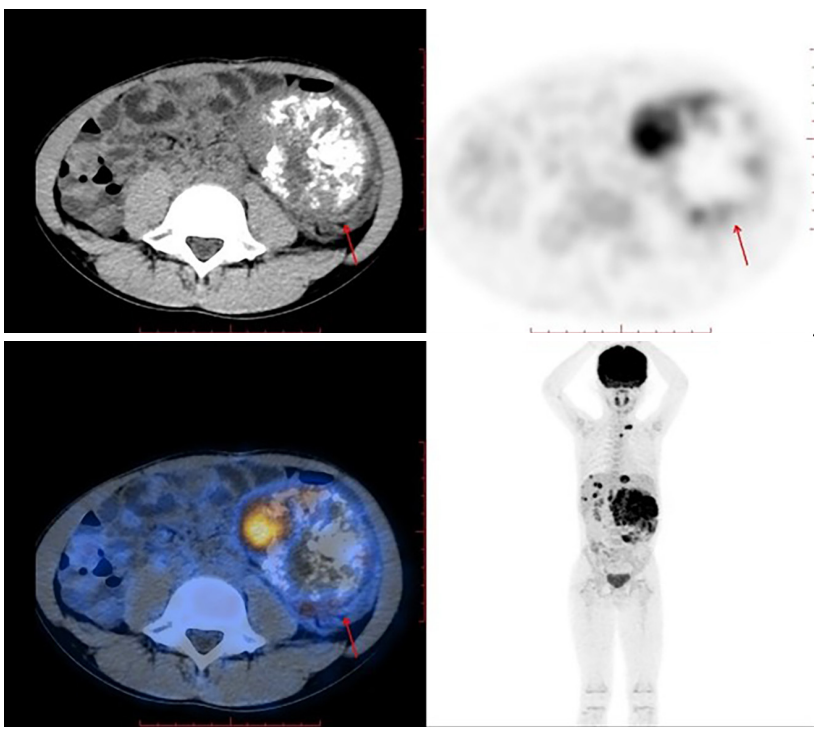

Figure 2 On PET-CT fusion images, the metabolic activity of the left kidney tumor (red arrows) was significantly increased, with an SUV_{max} of 10.2. In addition, multiple metastases in the liver and lymph node metastases around the lesion, abdominal cavity, mediastinum, and left supraclavicular fossa were detected, and radioactive concentrations were seen within them. PET, positron emission tomography; CT, computed tomography; SUV_{max}, maximum standardized uptake value.

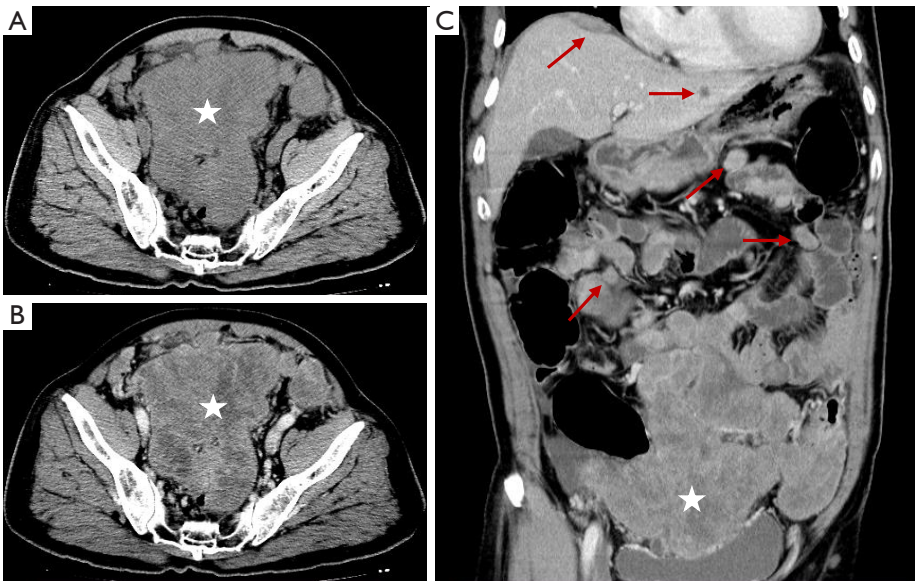

Figure 3 CT Results for case 2. (A,B) Irregular soft tissue masses (asterisks) were seen in the pelvic cavity, with uneven density and an indistinct boundary with the adjacent bowel. The plain CT value of the mass was about 24–29 HU, and the lesion showed moderate enhancement after the enhanced scan, with the CT value range of about 49–54 HU. (C) Coronal CT showed that the tumors (asterisk) were mainly located in the lower abdomen to the pelvic region. Multiple metastases were apparent in the liver, right diaphragm, and the mesenteric space (red arrows). CT, computed tomography.

mass with radioactive concentration and a maximum standardized uptake value (SUV_{max}) of approximately 10.2, which was considered malignant. Lymph node metastases were also found in the left supraclavicular fossa and upper mediastinum (*Figure 2*). During his hospitalization, the patient underwent a left-sided nephrectomy and microwave ablation of liver metastases, after which he underwent a series of chemotherapy treatments.

Case 2

A 66-year-old man was admitted to hospital after a physical examination revealed an abdominal mass for more than 2 weeks. He underwent an abdominal CT examination, which showed multiple intra-abdominal masses that were poorly demarcated from the bowel and revealed multiple lymph node metastases between the mesentery, as well as metastases in the splenic hilum and liver (*Figure 3*). Subsequently, a puncture biopsy of the mass was performed. After a period of symptomatic management, the patient voluntarily requested to be discharged.

Pathology

Two experienced pathologists (5 and 10 years of work experience) read the slides. The tumor sections of these 2 patients were grayish-yellow in color and soft to medium in texture. The pathological sections were stained with hematoxylin and eosin and observed under 100× and 200× microscopy, respectively. Microscopically, the small round tumor cells formed nests and sheets in the desmoplastic stroma, significant interstitial fibrous tissue hyperplasia with glassy degeneration, and occasionally chrysanthemum-like structures with visible patchy necrosis (*Figure 4*). Immunohistochemical results indicated that the tumor cells diffusely expressed cytokeratin (CK), vimentin, and desmin (paranuclear point), and epithelial membrane antigen (EMA; focal+) was positive in both cases, while neuron-specific enolase (NSE), MyoD1, myogenin, CD99, S100, CD3, CD20, and transducer-like enhancer of split 1 (TLE1) were all negative. In addition, genetic testing of the tumor was performed in case 1, which demonstrated a broken recombination of the Ewing sarcoma region 1 (*EWSR1*) gene and a positive fluorescence *in situ* hybridization (FISH) test. Overall, the final diagnosis was DSRCT.

Follow-up

In case 1, the child began follow-up from July 16, 2021,

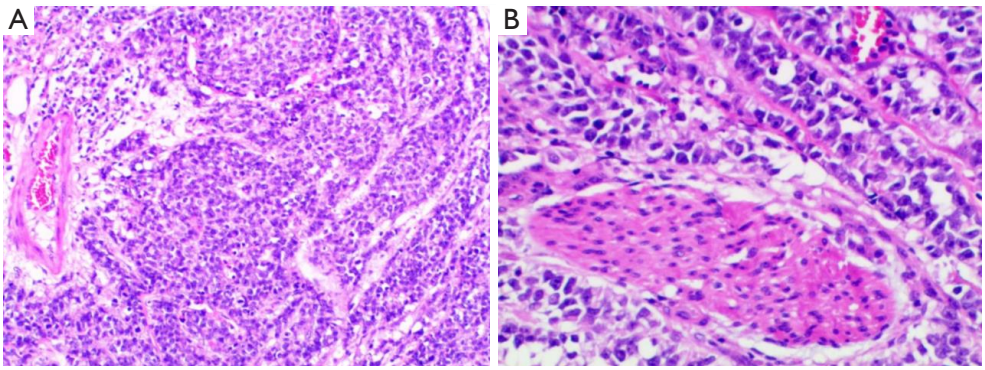

Figure 4 HE staining was performed on pathological sections. (A) The tumor cells appeared distributed in a nested or sheet-like pattern with sparse cell cytoplasm (HE 100×). (B) Tumor cells with sparse cytoplasm, visible nuclei, and involvement of nerve bundles (HE 200×). HE, hematoxylin and eosin.

which is continuing as of time of writing, and no definite tumor recurrence has been observed on abdominal CT examination for more than 1 year. Unfortunately, for case 2, no follow-up data have been obtained.

All procedures performed in this study were in accordance with the ethical standards of the institutional and/or national research committee(s) and with the Declaration of Helsinki (as revised in 2013). Verbal informed consent was obtained from the parent or legal guardian of the case 1 patient, and written informed consent was obtained from the case 2 patient for publication of this case report and accompanying images. A copy of the written consent is available for review by the editorial office of this journal.

Discussion

Desmoplastic small round cell tumor (DSRCT), first discovered in 1989 by Gerald and Rosai, is a rare malignancy in the small round cell family (11). DSRCT often occurs in adolescents and young men, the peritoneal cavity is the most common site, and usually spreads along the peritoneal surface (12,13). Clinical symptoms are nonspecific, mainly manifest as abdominal pain, bloating, or palpable abdominal masses (10,12). Most (~90%) cases of DSRCT are associated with diffuse or multifocal large omental and peritoneal lesions. Diaphragmatic involvement and retroperitoneal involvement are seen in 40% to 50% of cases, mainly in the form of tumor implantation and lymph node metastases, with additional liver metastases being relatively common (>30%) (10). In case 2, the patient presented with multiple abdominal masses and combined abdominal lymph nodes and liver metastases, which are consistent with the literature mentioned above. Moreover, this was an older adult patient, an age group in which DSRCT is rarer. In recent years, a small number of studies have compared adolescents and adults (≥18 years old) with DSRCT, but no significant differences in clinical manifestations, treatment methods, or prognoses between the 2 groups were found (14,15). The primary renal DSRCT was first reported in 2004 by Su *et al.* (16). Thus far, 19 cases of primary renal DSRCT have been reported in the literature (13,17), so we report our case 1 as the 20th case (*Table 1*). When it occurs in visceral organs (such as the kidney), it is radiologically and pathologically similar to other malignancies, making its diagnosis markedly challenging.

Conventional imaging modalities such as CT and magnetic resonance imaging (MRI) can provide good morphological information for DSRCT, while CT scanning is the most widely used and preferred diagnostic modality for initial diagnosis and follow-up evaluation (12,18). The characteristic imaging finding of DSRCT is multiple soft tissue masses in the abdomen and pelvis involving the omentum or mesentery without an exact organ of origin (1,2). The multiple larger nodular or lobulated masses often appear with heterogeneous density, similar to necrosis, cystic changes, and hemorrhage, displaying areas of nonenhancement. Punctate or amorphous calcifications may be observed in both the primary tumor and metastases (1,2,12,19). As described, numerous foci of calcification were observed on DSRCT of the left kidney in case 1 as well as within the intra-abdominal metastases. Weak contrast enhancement in some areas may be due to the fibrous component of the tumor (19). MRI helps to

Table 1 Literature review of desmoplastic small round cell tumor of the kidney

Authors	Cases (no.)	Age (years)	Sex	History	Treatment	F-UP (mo)	Outcome
Su *et al.*	1	41	Male	None	Radical nephrectomy	18	Alive with no evidence of disease
Egloff *et al.*	2	6	Female	Gross hematuria after abdominal trauma	Radical nephrectomy; adjuvant chemotherapy	9	Alive with no evidence of disease
Eaton and Cendron	3	7	Female	Intermittent gross hematuria following a fall	Radical nephrectomy	12	Alive with no evidence of disease
Collardeau-Frachon *et al.*	4	14	Female	Gross hematuria, fever, abdominal mass	Chemotherapy, radical nephrectomy	8	Alive with evidence of disease (lung and liver metastasis)
Wang *et al.*	5	7	Female	Not stated	Nephrectomy, chemotherapy	24	Alive with no evidence of disease
Wang *et al.*	6	6	Female	Not stated	Nephrectomy, chemotherapy	32	Pulmonary metastasis at 32 mo with subsequent chemotherapy and stem cell transplant; disease-free 12 mo later
Wang *et al.*	7	6	Female	Not stated	Nephrectomy, chemotherapy	22	Alive with no evidence of disease
Wang *et al.*	8	8	Male	Not stated	Nephrectomy, chemotherapy	20	Recurrent intra-abdominal and hepatic disease at 20 mo with subsequent chemotherapy; currently stable
Da Silva *et al.*	9	10	Male	Abdominal pain, hematuria	Radical nephrectomy, radiation therapy, chemotherapy	12	Alive with disease (liver, lung, and bone metastasis)
Janssens *et al.*	10	14	Female	Pain, abdominal mass	Clinical Dx: WT, RCC; no surgery	Not stated	Not stated
Popov *et al.*	11	14	Not stated	Not stated	Not stated	Not stated	Not stated
Tagarelli *et al.*	12	21	Female	Not stated	Nephrectomy, chemotherapy/radiation therapy	31	Alive with disease (peritoneal metastasis)
Rao *et al.*	13	20	Male	Not stated	Nephrectomy	24	Dead of disease
Eklund *et al.*	14	7	Male	Gross hematuria, back pain	Nephrectomy, chemotherapy	Not stated	Not stated
Walton and Flores	15	6	Male	Pain related to facial bone metastasis	Nephrectomy, chemotherapy	Not stated	Not stated
Baydar *et al.*	16	7	Female	Abdominal pain	Chemotherapy, nephrectomy	30	Dead of disease
Galliani *et al.*	17	15	Male	Gross hematuria, mid-back to left flank pain	Radical nephrectomy, chemotherapy/radiation therapy	48	Dead of disease
Liu and Ya	18	40	Female	Cough, sputum, dyspnea	Chemotherapy	Not stated	Not stated
Asadbeigi *et al.*	19	22	Male	Right flank pain	Radical nephrectomy	Not stated	Not stated
Present case	20	9	Male	Palpable abdominal mass	Nephrectomy, chemotherapy	14	Alive with disease (liver and spine metastasis)

mo, month; Dx, diagnosis; WT, Wilms tumor; RCC, renal cell carcinoma; F-UP, follow-up.

determine the extent of the disease (2). On MRI, DSRCT has been reported to exhibit inhomogeneous isointensity or hypointensity on T1-weighted images compared to skeletal muscle and inhomogeneous hyperintensity on T2-weighted images (2,7,12). Nonetheless, some solid components of tumor show relative hypointensity on T2-weighted images, possibly due to dense cellular and desmoplastic response (20).

PET-CT usually shows multiple intraperitoneal hypermetabolic masses with a variable SUV_{max} of the masses, often up to 12, indicating a strong hypermetabolic trend (10). PET-CT may be superior to other imaging modalities in detecting occult lesions and monitoring recurrence due to the advantages of functional imaging (1,12,21). The PET-CT scan of case 1 clearly revealed distant left supraclavicular fossa and mediastinal lymph node metastases in addition to CT-visible intra-abdominal metastases. This helped to determine the extent of the lesion and clinical staging.

The diagnosis of DSRCT relies on pathology and immunohistochemistry. Histopathological examination demonstrates nests, cords, and sheets of small round cells embedded in the desmoplastic stroma. Immunological phenotyping shows the multidirectional differentiation of tumor cells, which can express a variety of immunophenotypes including epithelial (EMA and keratin), neural (NSE), and mesenchymal (vimentin and desmin) markers (20,22). The human Wilms tumor gene (*WTI*) was originally discovered as a tumor-suppressor gene, and it may play an important role in angiogenesis, the occurrence of metastasis, and the suppression of immune responses. Recent studies have found that *WTI* has potential carcinogenic effects in a variety of malignant tumors. DSRCT is characterized by chromosomal translocations that result in gene fusion involving *EWSR1* and Wilms tumor 1 (*WT1*) (13,23). Therefore, the EWS-WT1 fusion gene has high sensitivity and specificity for the diagnosis of DSRCT (24). The molecular test results of case 1 demonstrated a broken recombination in the *EWSR1* gene, which helped to confirm the diagnosis of DSRCT.

The differential diagnosis of DSRCT is challenging, as diffusely spreading tumors such as desmoid tumors, malignant peritoneal mesothelioma, lymphoma, peritoneal sarcoma, gastrointestinal mesenchymal tumors, and Castleman disease can mimic DSRCT (25). However, they generally develop at an older age (19). In addition, malignant mesothelioma may involve a history of asbestos exposure; tends to occur in the pleura, peritoneum, and greater omentum; and is often associated with thoraco-abdominal fluid. Lymphoma is often associated with greater retroperitoneal lymph node enlargement but rarely calcification; meanwhile, desmoid tumor is a benign proliferation of fibrous tissue of the musculotendinous membrane that occurs mainly in women (26,27). Renal DSRCT in children needs to be differentiated from other renal malignancies, including Wilms tumor, rhabdoid tumor, and clear cell sarcoma. Clear cell sarcoma and rhabdoid tumor show almost no calcification. Although <15% of Wilms tumors in children may have calcifications, these calcifications are usually curvilinear in appearance and can be distinguished from the patchy and speckled calcifications found in DSRCT (28). In addition, the incidence of Wilms tumor and renal clear cell sarcoma peaks between 2 and 3 years of age, and rhabdoid tumors occur in infancy; however, in the bulk of the reports on pediatric renal DSRCT, this occurs above 6 years old, and thus this epidemiological feature can also assist in identification (29,30).

At present, there is no standard treatment protocol for DSRCT, and complete surgical resection of DSRCT is crucial when technically feasible (13). For most patients in advanced stages, effective systemic chemotherapy helps in systemic control (31). Other studies have shown that hyperthermic intraperitoneal chemotherapy (HIPEC) after cytoreductive surgery (CRS) is an effective local control method and can improve the survival rate of patients with DSRCT (32,33). Despite advances in multimodal therapy, patients with DSRCT have a poor prognosis, with about 60–70% dying from the disease within 2–3 years (34,35).

Conclusion

DSRCT is a rare disease commonly seen in children or adolescents with certain radiological features. By integrating morphology, immunohistochemistry, and molecular genetics, DSRCT can be accurately diagnosed. Despite aggressive treatment, the outcome remains poor. Clinical vigilance, identification, and multimodal therapy are required to improve patient prognosis.

Acknowledgments

Funding: This work was supported by National Natural Science Foundation Cultivation Project of the Third Affiliated Hospital of Sun Yat-sen University (No. 2021GZRPYMS06) and Five-Five Project of the Third Affiliated Hospital of Sun Yet-Sen University (No. 2023WW605).

Footnote

Conflicts of Interest: All authors have completed the ICMJE uniform disclosure form (available at https://qims.amegroups.com/article/view/10.21037/qims-22-1344/coif). The authors have no conflicts of interest to declare.

Ethical Statement: The authors are accountable for all aspects of the work in ensuring that questions related to the accuracy or integrity of any part of the work are appropriately investigated and resolved. All procedures performed in this study were in accordance with the ethical standards of the institutional and/or national research committee(s) and with the Helsinki Declaration (as revised in 2013). Verbal informed consent was obtained from the parent or legal guardian of the case 1 patient, and written informed consent was obtained from the case 2 patient for publication of this case report and accompanying images. A copy of the written consent is available for review by the editorial office of this journal.

References

1. Arora VC, Price AP, Fleming S, Sohn MJ, Magnan H, LaQuaglia MP, Abramson S. Characteristic imaging features of desmoplastic small round cell tumour. Pediatr Radiol 2013;43:93-102.
2. Kis B, O'Regan KN, Agoston A, Javery O, Jagannathan J, Ramaiya NH. Imaging of desmoplastic small round cell tumour in adults. Br J Radiol 2012;85:187-92.
3. Ariza-Prota MA, Pando-Sandoval A, Fole-Vázquez D, Casan P. Desmoplastic small round cell tumor of the lung: A case report and literature review. Respir Med Case Rep 2015;16:112-6.
4. Hatanaka KC, Takakuwa E, Hatanaka Y, Suzuki A, IIzuka S, Tsushima N, Mitsuhashi T, Sugita S, Homma A, Morinaga S, Hashegawa T, Matsuno Y. Desmoplastic small round cell tumor of the parotid gland-report of a rare case and a review of the literature. Diagn Pathol 2019;14:43.
5. George S, Vaideeswar P, Pandit S, Kane S, Khandeparkar J. Malignant small round cell tumor of the heart: a diagnostic dilemma. Cardiovasc Pathol 2007;16:56-8.
6. Huang J, Sha L, Zhang H, Tang X, Zhang X. Desmoplastic small round cell tumor in transverse colon: report of a rare case. Int Surg 2015;100:809-13.
7. Xuesong D, Hong G, Weiguo Z. Primary desmoplastic small round cell tumor of the tibia: PET/CT and MRI presentation of a rare case and review of the literature. J Bone Oncol 2019;20:100272.
8. Zhang GM, Zhu Y, Gan HL, Ye DW. Testicular desmoplastic small round cell tumor: a case report and review of literature. World J Surg Oncol 2014;12:227.
9. Vujić G, Mikuš M, Matak L, Bonevski A, Babić I, Planinić P, Babić D, Ćorušić A. Desmoplastic Small Round Cell Tumor of the Ovary: A Case Report with a New Modality of Treatment and Review of the Literature. Rev Bras Ginecol Obstet 2020;42:297-302.
10. Morani AC, Bathala TK, Surabhi VR, Yedururi S, Jensen CT, Huh WW, Prasad S, Hayes-Jordan A. Desmoplastic Small Round Cell Tumor: Imaging Pattern of Disease at Presentation. AJR Am J Roentgenol 2019;212:W45-54.
11. Gerald WL, Rosai J. Case 2. Desmoplastic small cell tumor with divergent differentiation. Pediatr Pathol 1989;9:177-83.
12. Zhang WD, Li CX, Liu QY, Hu YY, Cao Y, Huang JH. CT, MRI, and FDG-PET/CT imaging findings of abdominopelvic desmoplastic small round cell tumors: correlation with histopathologic findings. Eur J Radiol 2011;80:269-73.
13. Galliani CA, Bisceglia M, Del Giudice A, Cretì G. Desmoplastic Small Round Cell Tumor of the Kidney: Report of a Case, Literature Review, and Comprehensive Discussion of the Distinctive Morphologic, Immunohistochemical, and Molecular Features in the Differential Diagnosis of Small Round Cell Tumors Affecting the Kidney. Adv Anat Pathol 2020;27:408-21.
14. Olivier-Gougenheim L, Orbach D, Atallah V, Marec-Berard P, Bertrand A. Desmoplastic Small Round Cell Tumors With EWS-WT1 Transcript Expression: Should We Consider Children and Adult Patients Differently? J Pediatr Hematol Oncol 2022;44:e637-42.
15. Lettieri CK, Garcia-Filion P, Hingorani P. Incidence and outcomes of desmoplastic small round cell tumor: results from the surveillance, epidemiology, and end results database. J Cancer Epidemiol 2014;2014:680126.
16. Su MC, Jeng YM, Chu YC. Desmoplastic small round cell

tumor of the kidney. Am J Surg Pathol 2004;28:1379-83.
17. Liu Y, Tao Y, Wang F, Huang Z. Desmoplastic Small Round Cell Tumor of the Kidney With Mainly Pulmonary Symptoms by (18)F-FDG PET/CT. Urology 2021;154:e15-6.
18. Li G, Wang HT, Gao Y, Cui XJ, Zhang GZ. Primary abdominopelvic desmoplastic small round cell tumor: CT and correlated clinicopathologic features. Eur Rev Med Pharmacol Sci 2014;18:2670-7.
19. Chouli M, Viala J, Dromain C, Fizazi K, Duvillard P, Vanel D. Intra-abdominal desmoplastic small round cell tumors: CT findings and clinicopathological correlations in 13 cases. Eur J Radiol 2005;54:438-42.
20. Gorospe L, Gómez T, González LM, López A. Desmoplastic small round cell tumor of the pelvis: MRI findings with histopathologic correlation. Eur Radiol 2007;17:287-8.
21. Thomas R, Rajeswaran G, Thway K, Benson C, Shahabuddin K, Moskovic E. Desmoplastic small round cell tumour: the radiological, pathological and clinical features. Insights Imaging 2013;4:111-8.
22. Ertoy Baydar D, Armutlu A, Aydin O, Dagdemir A, Yakupoglu YK. Desmoplastic small round cell tumor of the kidney: a case report. Diagn Pathol 2020;15:95.
23. Salvatorelli L, Calabrese G, Parenti R, Vecchio GM, Puzzo L, Caltabiano R, et al. Immunohistochemical Expression of Wilms' Tumor 1 Protein in Human Tissues: From Ontogenesis to Neoplastic Tissues. Applied Sciences 2019;10:40.
24. Rekhi B, Ahmed S, Basak R, Qureshi SS, Desai SS, Ramadwar M, Desai SB, Kurkure P, Jambhekar NA. Desmoplastic small round cell tumor-clinicopathological spectrum, including unusual features and immunohistochemical analysis of 45 tumors diagnosed at a tertiary cancer referral centre, with molecular results t(11; 22) (p13; q12) (EWS-WT1) in select cases. Pathol Oncol Res 2012;18:917-27.
25. Levy AD, Arnáiz J, Shaw JC, Sobin LH. From the archives of the AFIP: primary peritoneal tumors: imaging features with pathologic correlation. Radiographics 2008;28:583-607; quiz 621-2.
26. Iyer RS, Schaunaman G, Pruthi S, Finn LS. Imaging of pediatric desmoplastic small-round-cell tumor with pathologic correlation. Curr Probl Diagn Radiol 2013;42:26-32.
27. Bellah R, Suzuki-Bordalo L, Brecher E, Ginsberg JP, Maris J, Pawel BR. Desmoplastic small round cell tumor in the abdomen and pelvis: report of CT findings in 11 affected children and young adults. AJR Am J Roentgenol 2005;184:1910-4.
28. Egloff AM, Lee EY, Dillon JE, Callahan MJ. Desmoplastic small round cell tumor of the kidney in a pediatric patient: sonographic and multiphase CT findings. AJR Am J Roentgenol 2005;185:1347-9.
29. Wang LL, Perlman EJ, Vujanic GM, Zuppan C, Brundler MA, Cheung CR, Calicchio ML, Dubois S, Cendron M, Murata-Collins JL, Wenger GD, Strzelecki D, Barr FG, Collins T, Perez-Atayde AR, Kozakewich H. Desmoplastic small round cell tumor of the kidney in childhood. Am J Surg Pathol 2007;31:576-84.
30. Tagarelli A, Spreafico F, Ferrari A, Alaggio R, Cecchetto G, Collini P, Indolfi P, Burnelli R, Morali L, Bisogno G. Primary renal soft tissue sarcoma in children. Urology 2012;80:698-702.
31. Ambar NBD, de Seixas Alves MT, Lederman HM, Abib S, Duarte AAB, Caran EM. Irinotecan and vincristine for the treatment of refractory desmoplastic small round cell tumor in a developing country: a case report. J Med Case Rep 2019;13:77.
32. Hayes-Jordan AA, Coakley BA, Green HL, Xiao L, Fournier KF, Herzog CE, Ludwig JA, McAleer MF, Anderson PM, Huh WW. Desmoplastic Small Round Cell Tumor Treated with Cytoreductive Surgery and Hyperthermic Intraperitoneal Chemotherapy: Results of a Phase 2 Trial. Ann Surg Oncol 2018;25:872-7.
33. Stiles ZE, Murphy AJ, Anghelescu DL, Brown CL, Davidoff AM, Dickson PV, Glazer ES, Bishop MW, Furman WL, Pappo AS, Lucas JT Jr, Deneve JL. Desmoplastic Small Round Cell Tumor: Long-Term Complications After Cytoreduction and Hyperthermic Intraperitoneal Chemotherapy. Ann Surg Oncol 2020;27:171-8.
34. Jayakrishnan T, Moll R, Sandhu A, Sanguino A, Kaur G, Mao S. Desmoplastic Small Round-cell Tumor: Retrospective Review of Institutional Data and Literature Review. Anticancer Res 2021;41:3859-66.
35. Stiles ZE, Dickson PV, Glazer ES, Murphy AJ, Davidoff AM, Behrman SW, Bishop MW, Martin MG, Deneve JL. Desmoplastic small round cell tumor: A nationwide study of a rare sarcoma. J Surg Oncol 2018;117:1759-67.

Cite this article as: Chen W, Chen H, Zhao C, Xie S, Qin J, Liu W. Desmoplastic small round cell tumor: the report of two cases and literature analysis review of the radiological findings. Quant Imaging Med Surg 2023;13(7):4762-4769. doi: 10.21037/qims-22-1344

